

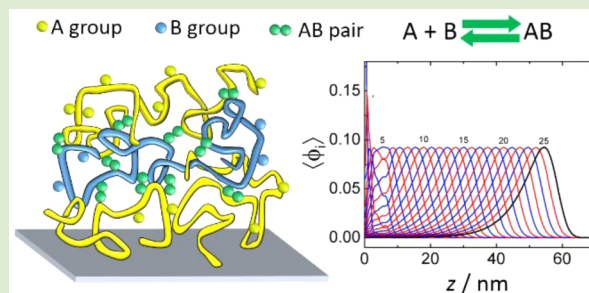
## Layer-by-Layer Self-Assembly of Polymers with Pairing Interactions

Gervasio Zaldivar and Mario Tagliacruz\*

INQUIMAE-CONICET and DQIAQF, University of Buenos Aires, School of Sciences, Ciudad Universitaria, Pabellón 2, Ciudad Autónoma de Buenos Aires C1428EHA, Argentina

## Supporting Information

**ABSTRACT:** A molecular theory is introduced to model the layer-by-layer self-assembly (LbL-SA) of polymers with pairing interactions. Our theory provides a general framework to describe nonelectrostatic LbL-SA as the pairing interactions generically describe the formation of bonds between two complementary chemical species, for example, hydrogen donor and acceptor in hydrogen-bonding-LbL or host and guest in host-guest-LbL. The theory predicts fundamental observations related to LbL-SA: (i) phase separation of a mixture of polymers with pairing interactions in bulk solution, (ii) linear increase in film thickness with the number of LbL adsorption steps, (iii) stoichiometry over-compensation after each adsorption step, and (iv) interpenetration of polymer layers. Importantly, this study shows that the minimal requirement for nonelectrostatic LbL is the competition of a pairing interaction and an excluded-volume repulsion. A simple analytical model based on this competition predicts the volume fraction of the layers in good agreement with the numerical predictions of the molecular theory.



Layer-by-layer self-assembly (LbL-SA) is one of the most versatile and widespread tools to modify surfaces with thin polymer films.<sup>1</sup> The first implementations of the technique involved the sequential adsorption of a polyanion and a polycation,<sup>2,3</sup> but later investigations demonstrated LbL-SA of polymers interacting via nonelectrostatic forces,<sup>4</sup> such as hydrogen bonds,<sup>5–7</sup> halogen bonds,<sup>8</sup> charge transfer,<sup>9</sup> biomolecular recognition,<sup>10</sup> and host–guest interactions.<sup>11</sup>

Despite the great scientific and technological success of LbL-SA, open questions remain about the fundamental mechanisms of sequential polymer adsorption. In the case of polyelectrolyte multilayers, these mechanisms have been explored by theory<sup>12–17</sup> and simulations,<sup>16,18–20</sup> although some aspects of multilayer build-up are still under discussion.<sup>16</sup> On the other hand, to the best of our knowledge, there is a lack of theoretical work devoted to nonelectrostatic LbL.

We present here a theory for nonelectrostatic LbL that generically describes the interactions responsible for polymer pairing as association reactions:



where A and B are the groups located in the polymers that are involved in the pairing interaction. For example, A and B can be a hydrogen donor and a hydrogen acceptor in H-bonding-LbL. They can also be a donor and acceptor of halogen in halogen-bonding-LbL or of electron density in charge-transfer-LbL, as well as chemical groups with complementary biological recognition in biorecognition-mediated LbL or a host and a guest in host-guest-LbL.

Our theoretical strategy to model LbL-SA follows the same procedure as the experiment, namely: (i) we model the

adsorption of poly-A (i.e., the polymer with A-type segments) on a substrate coated by B-type monomers, (ii) we perform a “rinsing” step, where the chains of poly-A that are involved in less than a certain number of AB contacts are removed from the system, and (iii) we repeat steps i and ii, alternating the adsorption of poly-A and poly-B until the desired number of layers is deposited. In order to model the adsorption steps, we developed a theoretical approach based on the combination of a molecular theory developed by Szeleifer and collaborators<sup>21,22</sup> for soft materials at interfaces and the theory of associative polymers of Semenov and Rubinstein<sup>23,24</sup> that we modified here for the association between two different types of polymers instead of the self-association of a single type of polymer. Our theory requires writing down and minimizing a free energy functional of the system. This approach assumes that the adsorption of the polymer in solution reaches equilibrium in the time scale of the adsorption step (10–20 min), which is supported by kinetic experiments that show that such a time scale is usually long enough to ensure saturation of the amount of adsorbed polymer.<sup>25,26</sup>

The free-energy functional,  $F$ , for the adsorption of poly-A on a previously deposited poly-A/poly-B film is

Received: March 31, 2016

Accepted: June 28, 2016

$$\begin{aligned} \frac{\beta F}{A} &= \int \rho_s(z) [\ln(\rho_s(z)v_s) - 1] dz \\ &+ \int \rho_A(z) [\ln(\rho_A(z)v_s) - 1] dz \\ &+ \int \rho_A(z) \left[ \sum_{\alpha} P_A(\alpha, z) \ln P_A(\alpha, z) \right] dz + \frac{\beta F_{\text{pair}}}{A} \end{aligned} \quad (2)$$

In this expression,  $\beta = 1/k_B T$  and  $z$  is the distance from the plane of the substrate. We assume that our system is homogeneous in the  $x$ - $y$  plane and, therefore, all functions in our theory depend on  $z$  but not on  $x$  and  $y$ . The first two terms in eq 2 account for the translational entropies of the solvent and poly-A chains in solution, respectively. In these terms,  $\rho_s(z)$  and  $\rho_A(z)$  are the number densities of solvent molecules and poly-A chains at  $z$ , respectively, and  $v_s$  is the molecular volume of the solvent. The third term in eq 2 is the free-energy contribution due to the configurational entropy of poly-A chains, where  $P_A(\alpha, z)$  is the probability of having a poly-A chain in conformation  $\alpha$  that has its first segment at  $z$  and the sum runs over all possible conformations of poly-A chains. The last contribution to  $F$  is the free energy of formation of AB pairs. This contribution, derived in the Supporting Information (SI), is

$$\begin{aligned} \frac{\beta F_{\text{pair}}}{A} &= \int \langle n_A(z) \rangle f_A(z) \beta \Delta E_{\text{pair}}^0 dz \\ &+ \int \langle n_A(z) \rangle [(1 - f_A(z)) (\ln(1 - f_A(z))) \\ &+ f_A(\ln(f_A(z)))] dz \\ &+ \int \langle n_B(z) \rangle [(1 - f_B(z)) (\ln(1 - f_B(z))) \\ &+ f_B(\ln(f_B(z)))] dz \\ &- \int \langle n_A(z) \rangle f_A(z) (\ln(\langle n_A(z) \rangle f_A(z) v_{\text{AB}}) - 1) dz \end{aligned} \quad (3)$$

where  $f_i(z)$  ( $i = A, B$ ) is the fraction of groups of type  $i$  at  $z$  forming an AB pair,  $\langle n_i(z) \rangle$  is the total concentration of monomers of type  $i$  at  $z$ , which has contributions both from the polymer being adsorbed and the polymer chains already adsorbed in previous layers, and  $\Delta E_{\text{pair}}^0$  and  $v_{\text{AB}}$  are the energy of formation and the volume of the AB pair, respectively. The first term in eq 3 is the free energy of formation of single, isolated AB pair at  $z$ , the next two terms correspond to the mixing entropies of free and bound A-type and B-type monomers and they are similar to those found for acid–base equilibria.<sup>22</sup> The last term arises from the fact that the two species involved in the pairing equilibrium, A and B, are located on the polymer chains and not free in solution. This contribution is absent in the case of acid–base equilibrium, which involves the reaction of a group on the polymer with a proton or hydroxyl ion free in solution.<sup>22</sup> It is worthwhile to mention that acid–base equilibrium involves binding between a small molecule and an acid–base group in the chain and, therefore, it is different from donor–acceptor binding between chains, where chain connectivity may introduce correlations between binding events. However, in our mean-field description of the problem these correlations are omitted, thus acid–base and donor–acceptor equilibrium are described by similar (but not exactly equivalent) expressions. This mean-field description of the problem is a good approximation for

dense systems, where each polymer segment interacts not only with segments of the same chain but also with segments in multiple neighboring chains and the system is approximately homogeneous in planes parallel to the substrate. Since multilayer polymer films are rather dense systems, we believe that such mean-field description will be approximately valid.

The equilibrium state of the system results from the minimization of eq 2 with respect to  $\rho_A(z)$ ,  $\rho_s(z)$ ,  $f_A(z)$ ,  $f_B(z)$ , and  $P_A(\alpha, z)$  subjected to two constraints: (i) a packing constraint (the sum of the volume fraction of all species at each  $z$  is one), which accounts for and gives rise to the intermolecular excluded-volume repulsions in the theory (note that eq 2 does not contain an explicit term for repulsive interactions) and (ii) a stoichiometry constraint (the number of A-type and B-type segments at  $z$  involved in AB pairs is the same). We fix the density profiles of previously adsorbed layers during minimization, but AB bonds can still rearrange since we minimize  $F$  with respect to  $f_A(z)$  and  $f_B(z)$ . This approximation is based on the fact that each adsorbed chain is involved in several AB bonds, which restricts its translational and conformational degrees of freedom, and thus the approximation will be better for chains deep within the film than for those at the interface. In the future, we plan to study the possibility of allowing previously adsorbed layers to relax.

The equations resulting from the minimization of  $F$  are described in detail in the SI, but it is interesting to discuss here the expression resulting from the minimization with respect to  $f_A(z)$  and  $f_B(z)$ :

$$\frac{f_B(z) \langle n_B(z) \rangle}{(1 - f_A(z)) \langle n_A(z) \rangle (1 - f_B(z)) \langle n_B(z) \rangle} = C \frac{[\text{AB}(z)]}{[\text{A}(z)][\text{B}(z)]} = K^0 \quad (4)$$

In this expression,  $[\text{A}(z)]$ ,  $[\text{B}(z)]$ , and  $[\text{AB}(z)]$  are the molar concentrations at  $z$  of unbound A groups, unbound B groups and AB pairs, respectively,  $C$  is a constant required to change from number density to molar concentrations (see SI) and the constant  $K^0 = v_{\text{AB}} \exp(-\beta \Delta E_{\text{pair}}^0)$  is the equilibrium constant for the formation of AB pairs in bulk solution. Expression 4 is clearly the equilibrium equation for the pairing reaction eq 1 at  $z$ . Using the typical energy of a hydrogen bond,  $\Delta E_{\text{pair}}^0 \sim -10$  to  $-40$  kJ/mol<sup>27</sup> and  $v_{\text{AB}} \sim 1$  nm<sup>3</sup> results in typical  $K^0$  values of  $\sim 6 \times 10^1$  to  $1 \times 10^7$  nm<sup>3</sup> ( $K^0/C \sim 3 \times 10^1$  to  $6 \times 10^6$  M<sup>-1</sup>).

Following polymer adsorption, a rinsing step is required to remove the chains in the bulk as well as loosely bound polymers. To remove these chains, we first determine the average number of AB bonds for each poly-A chain in the system (see SI) and then we remove from the system those chains that have, on average, less than a certain number of bonds (in this work, we used a cutoff of one bond).

Solution mixtures of polymers with electrostatic interactions (i.e., polycation and polyanion)<sup>28</sup> or nonelectrostatic interactions (i.e., polymeric hydrogen acceptor and donor<sup>29</sup>) phase separate into a polymer-rich phase (known as coacervate in the case of polyelectrolytes<sup>28</sup>) and a solvent-rich phase. This phenomenon is usually related to the ability of the polymers to form LbL films,<sup>30,31</sup> therefore, it is interesting to examine first the predictions of our model for a mixture of poly-A and poly-B in bulk solution. We have studied the thermodynamic stability of this mixture using exactly the same free energy functional proposed in eq 2 for LbL-SA, with two main differences: (i) all functions in the bulk are independent of  $z$ , (ii) both polymers are present in the bulk, so a translational entropy term of poly-B should be also included. Our model of polymers with pairing interactions predicts phase separation of bulk solutions (see

SI). Figure 1 shows the phase diagram for a mixture of poly-A and poly-B as a function of  $K^0$ ,  $c_p$  (total molar concentration of

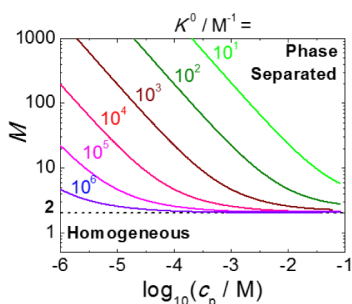


Figure 1. Phase diagram of a 1:1 mixture of poly-A and poly-B in homogeneous solution as a function of the total monomer concentration ( $c_p$ ) and the chain length ( $M$ ). The solid lines show the onset for phase separation for different values of the pairing constant,  $K^0$ . Above these lines, the homogeneous phase becomes thermodynamically unstable and the system must phase separate into a polymer-rich and a polymer-poor phase (i.e., the lines are spinodal lines).

polymer monomers in the bulk), and  $M$  (chain length) for a solution where the concentrations and chain lengths of both polymers are the same. Note that we did not consider polymer–solvent and polymer–polymer van der Waals attractions in the present theory, thus the polymers are in good-solvent conditions and they are attracted only by the pairing interaction. We observe that phase separation is favored by increasing  $K^0$  and  $M$ , which has an origin in the competition between the translational entropy of the chains (higher translational entropy favors the homogeneous system) and the free energy of formation of AB bonds (which favors phase separation). For a fixed concentration of polymer chains, the translational entropy is independent of  $K^0$  and  $M$ , but the pairing free energy becomes more negative for increasing  $K^0$  and  $M$ , which explains the effect of these variables on the phase diagram of Figure 1. Another interesting prediction of our theory is that phase separation is impossible for  $M \leq 2$  (dashed line in Figure 1), which is consistent with the well-established fact that small molecules cannot be, in general, deposited by LbL-SA.

We now focus our attention back to LbL-SA. Our theory predicts film growth by sequential adsorption of poly-A and poly-B in a broad range of conditions. For example, Figure 2a shows the volume fraction profiles,  $\langle \phi_j(z) \rangle = \langle n_j(z) \rangle v_p$  (where  $j$  denotes the layer number and  $v_p$  is the volume of a segment) for each of the polymer layers within a 20-layer film, where the first layer is poly-A and the last layer is poly-B. After a few initial layers, the profiles show all the same shape, but are progressively displaced away from the surface as the layer number increases. Note also the high degree of interpenetration between layers, in qualitative agreement with experimental observations.<sup>32,33</sup> Figure 2b shows that the film thickness (defined as the first moment of the polymer volume fraction, see SI) increases linearly with the number of adsorption steps after an initial nonlinear growth in the first  $\sim 8$  layers. Linear growth has been experimentally observed in LbL-SA based on hydrogen bonds,<sup>5</sup> halogen bonds,<sup>8</sup> and charge-transfer interactions.<sup>9</sup>

Figure 3a shows the total volume fractions of poly-A and poly-B in the film, that is, the sum of the volume fractions of all poly-A and of all poly-B layers, respectively, as a function of the

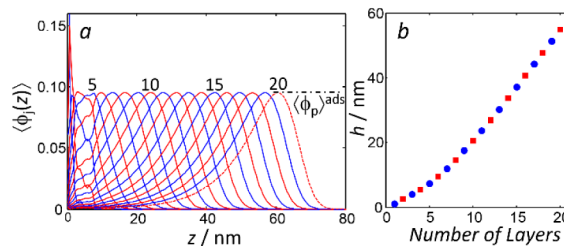


Figure 2. (a) Predicted volume fraction of layer  $j$ ,  $\langle \phi_j \rangle$ , as a function of the distance from the substrate for the LbL adsorption of 20 layers (terminated in poly-B). Blue and red lines show the profiles for poly-A and poly-B layers, respectively. The dash-dotted line shows the maximum volume fraction of the individual layers,  $\langle \phi_p \rangle^{\text{ads}}$ . (b) Thickness of the film,  $h$ , as a function of the number of adsorbed layers. Calculation parameters:  $M = 100$  segments/chains; bulk polymer concentration = 1.5 mM (in monomer units; this concentration corresponds to a volume fraction of  $\langle \phi_p \rangle^{\text{bulk}} = 10^{-4}$ );  $K^0 = 1.1 \times 10^2 \text{ nm}^3$  ( $K^0/C = 7 \times 10^1 \text{ M}^{-1}$ ); surface density of B groups on the substrate surface,  $\sigma_B = 1.3 \text{ nm}^{-2}$ .

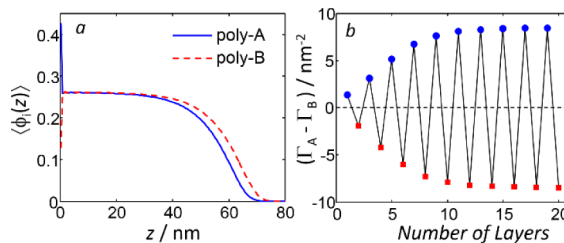


Figure 3. (a) Predicted total volume fraction of polymer type  $i$ ,  $\langle \phi_i \rangle$  ( $i = A$  or  $B$ ), as a function of the distance from the substrate for a 20-layer film. (b) Difference of the total surface coverages of poly-A,  $\Gamma_A$ , and poly-B,  $\Gamma_B$ , as a function of the number of adsorbed layers. The total surface coverage of  $i$  is obtained by integration of  $\langle \phi_i \rangle$  in the whole system ( $\Gamma_B$  contains as well a contribution of the B groups on the substrate surface). Same calculation conditions as in Figure 2.

distance to the substrate. The total volume fractions of poly-A and poly-B are exactly equal to each other in the central region of the film ( $z$  from  $\sim 1$  to  $\sim 30$  nm), but poly-A is enriched near the substrate/film interface and poly-B has a higher concentration at the film/solution interface. This structure is reminiscent to Decher's three-zone model of polyelectrolyte multilayers.<sup>1</sup> Figure 3b shows the difference of the total surface coverage of poly-A,  $\Gamma_A$ , and that of poly-B,  $\Gamma_B$  (i.e.,  $\Gamma_A - \Gamma_B$ , the surface excess of poly-A), as a function of the number of adsorbed layers. We observe that  $\Gamma_A - \Gamma_B$  oscillates around zero, and after the first  $\sim 8$  adsorbed layers, the amplitude of the oscillations is constant. In other words, there is a stoichiometric overcompensation following the adsorption of each polymer layer, which results in a steady-state growth of the film with the number of adsorbed layers.

The results in Figures 2 and 3 show that our theory captures the most prominent features of typical LbL growth: linear growth, stoichiometric overcompensation, interpenetration of neighboring layers, and the formation of three distinct regions in the film. Based on the main ideas behind our theory, we will propose next a simple argument to explain the mechanism of multilayer build up for polymers with pairing interactions and check its predictions against the numerical predictions of the molecular theory.

Let us consider again the adsorption of a poly-A layer onto a poly-B-capped LbL multilayer. In our theory, the chemical

potential of the poly-A chains (in a homogeneous system) is given by (see SI):

$$\beta\mu_A = \frac{1}{V} \frac{\partial \beta F}{\partial \rho_A} = \ln \left( \frac{\langle \phi_A \rangle v_s}{M v_p} \right) - \frac{M v_p}{v_s} \ln(\langle \phi_s \rangle) + M \ln(1 - f_A) \quad (5)$$

where  $V$  is the volume of the system,  $\langle \phi_i \rangle$  is the volume fraction of the species  $i$  ( $i = A, s$  for A-type monomers and solvent),  $v_s$  and  $v_p$  are the molecular volumes of the solvent molecules and a polymer segment, and we have used the relation  $\rho_A = \langle \phi_A \rangle / (M v_p)$ . The first term in eq 5 accounts for the translational entropy of the chains, and the second term for the excluded-volume repulsions and the third term for the pairing interactions. The third term is always more negative at the film/solution interface (where the fraction of bound A-type segments,  $f_A$ , is  $>0$ ) than in the solution (where  $f_A = 0$  because there are no B-type segments present). Since the polymers flow from regions of high chemical potential to regions of low chemical potential, the pairing contribution always leads to an increase in the number of chains at the interface. The increase in the number density of poly-A at the interface is counterbalanced by the first and second terms of eq 5, which are always more positive at the interface than in the bulk. Therefore, after a few initial adsorption steps, the volume fraction of each adsorbed layer will become independent of the number of layers due to the balance between pairing attractions, steric repulsions, and translational entropy. Equating the chemical potential of polymers chains at the interface with that in solution leads to the following analytical model (derived in the SI),

$$\ln \left( \frac{\langle \phi_p \rangle^{\text{ads}}}{\langle \phi_p \rangle^{\text{bulk}}} \right) + M \ln \left( \frac{1}{2} \right) - \frac{M v_p}{v_s} \ln \left( 1 - \frac{3}{2} \langle \phi_p \rangle^{\text{ads}} \right) = 0 \quad (6)$$

where  $\langle \phi_p \rangle^{\text{ads}}$  is the peak volume fraction of a newly adsorbed polymer layer (i.e., the maximum volume fraction of each layer during linear growth, see Figure 2a) and  $\langle \phi_p \rangle^{\text{bulk}}$  is the volume fraction of the polymer chains in the bulk. In the conditions of Figure 2 ( $M = 100$ ,  $\langle \phi_p \rangle^{\text{bulk}} = 10^{-4}$ ,  $v_p = 0.11 \text{ nm}^3$ ,  $v_s = 0.03 \text{ nm}^3$ ), the solution of eq 6 is  $\langle \phi_p \rangle^{\text{ads}} = 0.1$  in good agreement with the full numerical results shown in Figure 2a. This result suggests that the balance between steric repulsions and pairing attractions is responsible from stoichiometry overcompensation in our system. Figure 4 shows that eq 6 captures the effect of  $M$  and  $\langle \phi_A \rangle^{\text{bulk}}$  on  $\langle \phi_A \rangle^{\text{ads}}$  for different calculation conditions. This figure also shows that overcompensation can be increased by increasing  $M$  and  $\langle \phi_A \rangle^{\text{bulk}}$ .

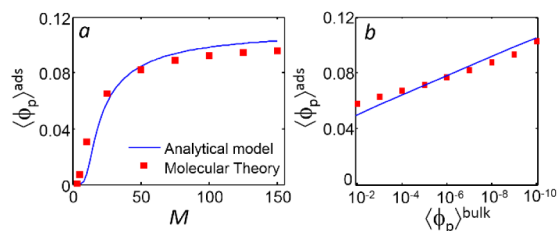


**Figure 4.** Maximum volume fraction of adsorbed layers,  $\langle \phi_p \rangle^{\text{ads}}$  (see Figure 2a) predicted by the analytical model (eq 6) and full molecular theory calculations as a function of (a) the chain length of the polymer,  $M$ , and (b) the volume fraction of the polymer in the bulk,  $\langle \phi_p \rangle^{\text{bulk}}$ . Calculation parameters:  $M = 50$  segments/chain (b);  $\langle \phi_p \rangle^{\text{bulk}} = 10^{-3}$  (a);  $K^0 = 1.1 \times 10^2 \text{ nm}^3$  ( $K^0/C = 7 \times 10^1 \text{ M}^{-1}$ );  $\sigma_B = 1.3 \text{ nm}^{-2}$ .

In summary, we have developed a molecular theory for polymers interacting via pairing attractions that successfully predicts both phase separation in bulk solutions and LbL-SA on a substrate. Our theory shows that nonelectrostatic LbL-SA can result from the competition of only two interaction forces: a generic pairing attraction (i.e., eq 1) and an excluded-volume steric repulsion. A main advantage of our model is its universal character, as the pairing eq 1 can represent different nonelectrostatic interactions, such as hydrogen-bonding, charge transfer, biomolecular recognition, host–guest interactions, and so on. Note that the association model given by eq 1 is the simplest possible. More advanced models for specific interactions will be explored in future work, for example, hydrogen-bonding models explicitly considering solvent-segment and solvent–solvent pairing.<sup>24</sup> Furthermore, Schlenoff and coworkers<sup>34,35</sup> and other groups<sup>36,37</sup> resorted to pairing interactions to describe the formation of ion pairs in electrostatic LbL and used this concept to explain diverse experimental findings about polyelectrolyte multilayers. We thus believe that the present approach may be even useful to model electrostatic LbL, provided that long-range electrostatic interactions can be consistently incorporated into the present theory. Future work will be devoted to explore these possibilities as well as to relax some of the assumptions in the formulation of the theory. These efforts will lead to a better understanding of the formation and behavior of electrostatic and nonelectrostatic LbL assemblies, which have a tremendous technological potential but still are, in many aspects, not fully understood.

## ■ ASSOCIATED CONTENT

### 📄 Supporting Information

The Supporting Information is available free of charge on the ACS Publications website at DOI: 10.1021/acsmacrolett.6b00258.

Derivation of the pairing contribution to the free energy (eq 3), minimization of the free-energy functional, analysis of polymer mixtures in bulk solution and derivation of eq 6 (PDF).

## ■ AUTHOR INFORMATION

### Corresponding Author

\*E-mail: mario@qi.fcen.uba.ar.

### Notes

The authors declare no competing financial interest.

## ■ ACKNOWLEDGMENTS

The authors gratefully acknowledge financial support from Agencia Nacional de Promoción Científica y Tecnológica (ANPCyT) (PICT-2015-0099). M.T. is grateful to Igal Szleifer and Rikkert Nap for enlightened discussions. The authors acknowledge CONICET and Argentina National System for High Performance Computing (SNCAD-MinCyT) for access to computer clusters at Centro de Cómputos de Alto Rendimiento (CONICET Rosario) and Centro de Simulación Computacional para Aplicaciones Tecnológicas (CONICET - Polo Científico Tecnológico). MT is a fellow of CONICET.

## ■ REFERENCES

(1) Decher, G.; Schlenoff, B. J. *Multilayer Thin Films*; Wiley-VCH: Weinheim, 2003.

- (2) Decher, G.; Hong, J. D.; Schmitt, J. *Thin Solid Films* **1992**, 210–211, 831–835.
- (3) Decher, G. *Science* **1997**, 277, 1232–1237.
- (4) Quinn, J. F.; Johnston, A. P. R.; Such, G. K.; Zelikin, A. N.; Caruso, F. *Chem. Soc. Rev.* **2007**, 36, 707–718.
- (5) Stockton, W. B.; Rubner, M. F. *Macromolecules* **1997**, 30, 2717–2725.
- (6) Wang, L.; Fu, Y.; Wang, Z.; Fan, Y.; Zhang, X. *Langmuir* **1999**, 15, 1360–1363.
- (7) Chi, L.; Fuchs, H. *Macromol. Rapid Commun.* **1997**, 18, 509.
- (8) Wang, F.; Ma, N.; Chen, Q.; Wang, W.; Wang, L. *Langmuir* **2007**, 23, 9540–9542.
- (9) Shimazaki, Y.; Mitsuishi, M.; Ito, S.; Yamamoto, M. *Langmuir* **1997**, 13, 1385–1387.
- (10) Johnston, A. P. R.; Mitomo, H.; Read, E. S.; Caruso, F. *Langmuir* **2006**, 22, 3251–3258.
- (11) Crespo-Biel, O.; Dordi, B.; Reinhoudt, D. N.; Huskens, J. *J. Am. Chem. Soc.* **2005**, 127, 7594–7600.
- (12) Wang, Q. *Soft Matter* **2009**, 5, 413–424.
- (13) Shafir, A.; Andelman, D. *Eur. Phys. J. E: Soft Matter Biol. Phys.* **2006**, 19, 155–162.
- (14) Castelnovo, M.; Joanny, J. F. *Langmuir* **2000**, 16, 7524–7532.
- (15) Park, S. Y.; Rubner, M. F.; Mayes, A. M. *Langmuir* **2002**, 18, 9600–9604.
- (16) Cerda, J. J.; Qiao, B.; Holm, C. *Soft Matter* **2009**, 5, 4412–4425.
- (17) Solis, F. J.; Olvera; De La Cruz, M. *J. Chem. Phys.* **1999**, 110, 11517–11522.
- (18) Messina, R. *Macromolecules* **2004**, 37, 621–629.
- (19) Patel, P. A.; Jeon, J.; Mather, P. T.; Dobrynin, A. V. *Langmuir* **2005**, 21, 6113–6122.
- (20) Narambuena, C. F.; Beltramo, D. M.; Leiva, E. P. M. *Macromolecules* **2007**, 40, 7336–7342.
- (21) Szleifer, I.; Carignano, M. A. *Adv. Chem. Phys.* **1996**, 94, 165–260.
- (22) Tagliacuzzi, M.; Olvera de la Cruz, M.; Szleifer, I. *Proc. Natl. Acad. Sci. U. S. A.* **2010**, 107, 5300–5305.
- (23) Semenov, A. N.; Rubinstein, M. *Macromolecules* **1998**, 31, 1373–1385.
- (24) Dormidontova, E. E. *Macromolecules* **2004**, 37, 7747–7761.
- (25) Kovacevic, D.; van der Burgh, S.; de Keizer, A.; Cohen Stuart, M. A. *Langmuir* **2002**, 18, 5607–5612.
- (26) Calvo, E. J.; Etchenique, R.; Pietrasanta, L.; Wolosiuk, A.; Danilowicz, C. *Anal. Chem.* **2001**, 73, 1161–1168.
- (27) Israelachvili, J. *Intramolecular and Surface Forces*; Academic Press: Amsterdam, 2011.
- (28) Spruijt, E.; Westphal, A. H.; Borst, J. W.; Cohen Stuart, M. A.; van der Gucht, J. *Macromolecules* **2010**, 43, 6476–6484.
- (29) Ikawa, T.; Abe, K.; Honda, K.; Tsuchida, E. *J. Polym. Sci., Polym. Chem. Ed.* **1975**, 13, 1505–1514.
- (30) Sukhishvili, S. A.; Kharlampieva, E.; Izumrudov, V. *Macromolecules* **2006**, 39, 8873–8881.
- (31) Mjahed, H.; Voegel, J.-C.; Chassepot, A.; Senger, B.; Schaaf, P.; Boulmedais, F.; Ball, V. *J. Colloid Interface Sci.* **2010**, 346, 163–171.
- (32) Bai, S.; Wang, Z.; Gao, J.; Zhang, X. *Eur. Polym. J.* **2006**, 42, 900–907.
- (33) Kharlampieva, E.; Kozlovskaya, V.; Ankner, J. F.; Sukhishvili, S. A. *Langmuir* **2008**, 24, 11346–11349.
- (34) Jaber, J. A.; Schlenoff, J. B. *J. Am. Chem. Soc.* **2006**, 128, 2940–2947.
- (35) Schlenoff, J. B.; Ly, H.; Li, M. *J. Am. Chem. Soc.* **1998**, 120, 7626–7634.
- (36) Tagliacuzzi, M.; Grumelli, D.; Calvo, E. J. *Phys. Chem. Chem. Phys.* **2006**, 8, 5086–5095.
- (37) Tagliacuzzi, M.; Grumelli, D.; Bonazzola, C.; Calvo, E. J. *J. Nanosci. Nanotechnol.* **2006**, 6, 1731–1740.